

## The relaxation of polymers with linear flexible chains of uniform length<sup>1)</sup>

M. Baumgaertel, A. Schausberger<sup>2)</sup> and H. H. Winter

University of Massachusetts, Amherst, Massachusetts, USA

**Abstract:** The analysis of dynamic mechanical data indicates that linear flexible polymer chains of uniform length follow a scaling relation during their relaxation, having a linear viscoelastic relaxation spectrum of the form  $H(\lambda) = n_1 G_N^0 \times (\lambda/\lambda_{\max})^{n_1}$  for  $\lambda \leq \lambda_{\max}$ . Data are well represented with a scaling exponent of about 0.22 for polystyrene and 0.42 for polybutadiene. The plateau modulus  $G_N^0$  is a material-specific constant and the longest relaxation time depends on the molecular weight in the expected way. At high frequencies, the scaling behavior is masked by the transition to the glassy response. Surprisingly, this transition seems to follow a Chambon-Winter spectrum  $H(\lambda) = C\lambda^{-n_2}$ , which was previously adopted for describing other liquid/solid transitions. The analysis shows that the Rouse spectrum is most suitable for low molecular-weight polymers  $M \approx M_c$ , and that the de Gennes-Doi-Edwards spectrum clearly predicts terminal relaxation, but deviates from the observed behavior in the plateau region.

**Key words:** Relaxation spectrum; monodisperse polymers; scaling; glass transition; plateau modulus; recoverable compliance

### 1. Introduction and background

The most simple polymer one might consider has linear flexible molecular chains, all of the same length (monodisperse). The chains should form a system free of any ordering transition (crystallization, phase separation). Relaxation occurs by motion of the macromolecules within the constraint of their surrounding molecules. Extensive progress has been made in finding ways to describe this relaxation phenomenon, and many details of the molecular motion processes are known [1–7]. Correlations could be made between molecular parameters and macroscopic properties, such as longest relaxation time, plateau modulus, and recoverable compliance. Between all this insight, it is somewhat aggravating that the relaxation spectrum of the linear flexible monodisperse (LFM) polymer has evaded all attempts at providing a quantitative description. This can be

seen by simply plotting the dynamic modulus, as predicted by a Rouse spectrum [1]

$$G(t) = g \sum_{i=1}^N e^{-ti^2/\lambda_{\max}}, \quad N \gg 1 \quad (1)$$

or by a GDE-spectrum [3, 4]

$$G(t) = g \sum_{i=1,3,5}^N i^{-2} e^{-ti^2/\lambda_{\max}}, \quad N \gg 1 \quad (2)$$

against measured relaxation moduli of nearly LFM polymers. In the formulas, the front factor  $g$  and the longest relaxation time  $\lambda_{\max}$  depend on molecular weight and temperature. In each case, the spectrum evolved from a model for the molecular motion. Molecular details are explained by the original authors. Here we want to focus on the shape of the spectrum. The large deviations between predicted and measured relaxation behavior initiated extensive attempts to mend the theory by including more and more details of possible molecular interactions [4].

<sup>1)</sup> Dedicated to Prof. Richard S. Stein on the occasion of his 65th birthday.

<sup>2)</sup> On sabbatical leave from the University of Linz, Austria.

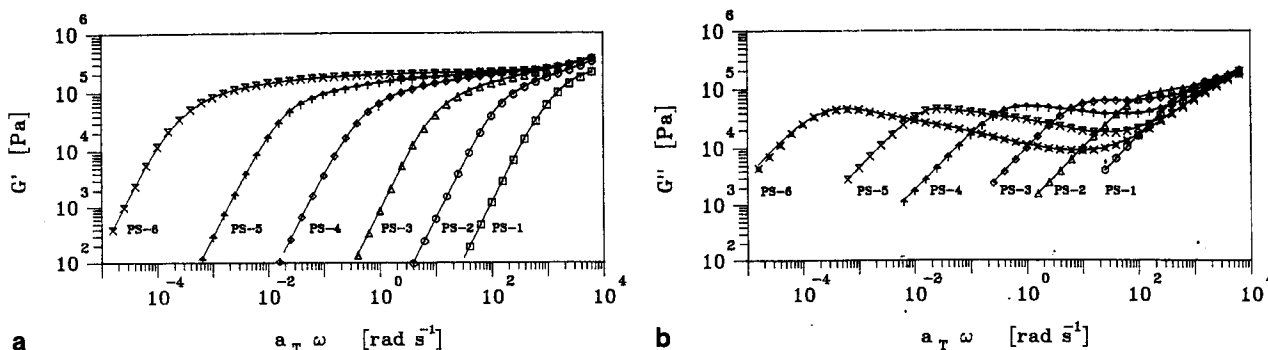


Fig. 1. Storage modulus a) and loss modulus b) of PS samples of Schausberger et al. [9]. The molecular weight and the polydispersity of the samples is PS-1:  $M_w = 34\,000$ ,  $M_w/M_N = 1.05$ ; PS-2:  $M_w = 65\,000$ ,  $M_w/M_N = 1.02$ ; PS-3:  $M_w = 125\,000$ ,  $M_w/M_N = 1.05$ ; PS-4:  $M_w = 292\,000$ ,  $M_w/M_N = 1.09$ ; PS-5:  $M_w = 757\,000$ ,  $M_w/M_N = 1.09$ ; PS-6:  $M_w = 2\,540\,000$ ,  $M_w/M_N = 1.13$ . The reference temperature is  $T_0 = 180^\circ\text{C}$

With this promising and, on the other hand, bothersome historical development in mind, we propose analyzing experimental data of (nearly) LFM polymers and abstracting them into a general picture. The relaxation spectrum of LFM polymers is expected to be very simple due to the highly idealized nature of the problem. This simplicity will make it possible to come to a solution.

Measured dynamic moduli of nearly LFM polymers are available in the literature [8–10]. We will use the data of Schausberger et al. [9] and Colby [10], because their data were made available to us in tabulated form (Figs. 1 and 2). The molecular parameters have been reported by the original authors. These experimental observations are necessarily biased by not being able to make a perfectly monodisperse polymer. For this reason, the polymers are termed nearly LFM polymers. In addition, the closeness to the glass transition alters the high fre-

quency side of  $G'(\omega)$ ,  $G''(\omega)$  in some unknown way. The data seem to be taken with great care, and possible systematic or statistical errors are considered to be small.

The data will be replicated by a standard (IRIS program) procedure [11], which chooses a discrete set of exponential decays:

$$G(t) = \sum_{i=1}^N g_i e^{-t/\lambda_i} \quad (3)$$

The discrete relaxation modes  $g_i$ ,  $\lambda_i$ ,  $i = 1, 2, \dots, N$ , as tabulated in Table 1, give an excellent fit of the data (see line through data in Figs. 1 and 2). All the experimental information is well represented by the discrete parameter set.

It is worth noting that no claim is made that the spectrum has to be discrete as compared to continuous. The result of this study will actually be a continuous spectrum, while the discrete representation is only an intermediate state in our analysis.

The following derivations will rely heavily on graphical methods. Therefore, an unusually large number of graphs will be needed. Also, we will use the word spectrum interchangeably for  $G(t)$  and for  $H(\lambda)$ , see Eq. (6) below.

## 2. Analysis of the discrete spectrum

The parameters of the discrete modes show a systematic pattern (Fig. 3). Within all the scatter, the short modes seem to group along a straight line of negative slope, while the long modes seem to follow a straight line of positive slope. This is a rather remarkable observation. Two basic relaxation processes are superimposed, and we are able to decouple them into a liquid like and a glassy contribution:

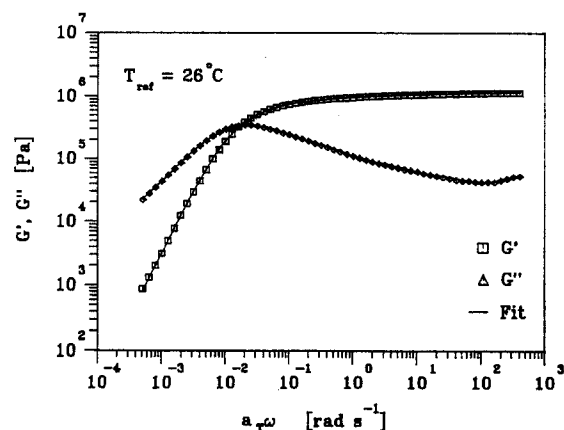


Fig. 2. Dynamic moduli of nearly monodisperse polybutadiene with  $M_w = 92\,500$ . The data were supplied by Dr. Ralph H. Colby from his PhD thesis [10]

Table 1. Discrete relaxation spectra of polystyrene standards PS-1...PS-6. The relaxation modes  $g_i$ ,  $\lambda_i$ ,  $i = 1, 2, \dots, N$  were calculated from the dynamic mechanical data (Fig. 1) using the IRIS program [11]

PS-1		PS-2	
$g_i$ [Pa]	$\lambda_i$ [s]	$g_i$ [Pa]	$\lambda_i$ [s]
$3.31 \cdot 10^4$	$1.56 \cdot 10^{-3}$	$9.57 \cdot 10^4$	$7.99 \cdot 10^{-3}$
$1.70 \cdot 10^5$	$5.10 \cdot 10^{-4}$	$9.12 \cdot 10^4$	$1.73 \cdot 10^{-3}$
$8.69 \cdot 10^5$	$2.57 \cdot 10^{-5}$	$1.13 \cdot 10^5$	$3.04 \cdot 10^{-4}$
		$5.26 \cdot 10^5$	$4.96 \cdot 10^{-5}$
PS-3		PS-4	
$g_i$ [Pa]	$\lambda_i$ [s]	$g_i$ [Pa]	$\lambda_i$ [s]
$6.40 \cdot 10^4$	$1.14 \cdot 10^{-1}$	$5.98 \cdot 10^3$	$5.79 \cdot 10^0$
$5.75 \cdot 10^4$	$3.32 \cdot 10^{-2}$	$6.30 \cdot 10^4$	$1.86 \cdot 10^0$
$4.64 \cdot 10^4$	$8.14 \cdot 10^{-3}$	$4.63 \cdot 10^4$	$4.80 \cdot 10^{-1}$
$5.95 \cdot 10^4$	$2.24 \cdot 10^{-3}$	$4.17 \cdot 10^4$	$1.07 \cdot 10^{-1}$
$8.32 \cdot 10^4$	$4.15 \cdot 10^{-4}$	$3.68 \cdot 10^4$	$1.94 \cdot 10^{-2}$
$5.05 \cdot 10^5$	$6.51 \cdot 10^{-5}$	$4.13 \cdot 10^4$	$3.06 \cdot 10^{-3}$
		$6.47 \cdot 10^4$	$5.55 \cdot 10^{-4}$
		$5.26 \cdot 10^5$	$6.92 \cdot 10^{-5}$
PS-5		PS-6	
$g_i$ [Pa]	$\lambda_i$ [s]	$g_i$ [Pa]	$\lambda_i$ [s]
$4.74 \cdot 10^3$	$1.68 \cdot 10^2$	$1.99 \cdot 10^4$	$7.79 \cdot 10^3$
$6.93 \cdot 10^4$	$4.81 \cdot 10^1$	$5.33 \cdot 10^4$	$2.66 \cdot 10^3$
$4.27 \cdot 10^4$	$8.86 \cdot 10^0$	$4.34 \cdot 10^4$	$7.37 \cdot 10^2$
$3.56 \cdot 10^4$	$1.52 \cdot 10^0$	$3.33 \cdot 10^4$	$1.36 \cdot 10^2$
$2.55 \cdot 10^4$	$2.87 \cdot 10^{-1}$	$2.44 \cdot 10^4$	$2.38 \cdot 10^1$
$1.75 \cdot 10^4$	$4.50 \cdot 10^{-2}$	$1.60 \cdot 10^4$	$4.21 \cdot 10^0$
$2.16 \cdot 10^4$	$5.98 \cdot 10^{-3}$	$1.04 \cdot 10^4$	$7.32 \cdot 10^{-1}$
$4.99 \cdot 10^4$	$8.06 \cdot 10^{-4}$	$8.64 \cdot 10^3$	$1.29 \cdot 10^{-1}$
$3.58 \cdot 10^5$	$1.05 \cdot 10^{-4}$	$9.24 \cdot 10^3$	$1.90 \cdot 10^{-2}$
		$2.53 \cdot 10^4$	$2.26 \cdot 10^{-3}$
		$9.52 \cdot 10^4$	$3.74 \cdot 10^{-4}$
		$1.01 \cdot 10^6$	$2.68 \cdot 10^{-5}$

$$G(t) = \underbrace{\sum_{i=1}^{N_1} g_{1,i} e^{-t/\lambda_{1,i}}}_{\text{flow regime}} + \underbrace{\sum_{i=1}^{N_2} g_{2,i} e^{-t/\lambda_{2,i}}}_{\text{glassy regime}} \quad (4)$$

The second observation is that the short modes of all polystyrene samples sit on the same line, while the long modes describe parallel lines, as sketched in Fig. 3 (i.e., same slope, but spaced out). The short modes are attributed to the glass transition, which is independent of molecular weight.

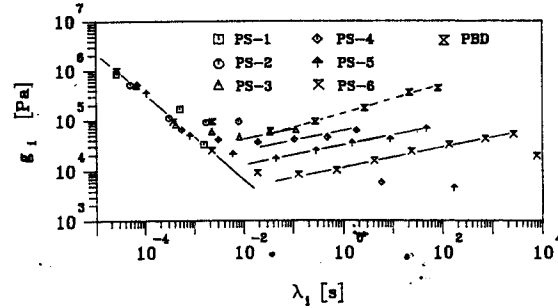


Fig. 3. Discrete relaxation spectra of the model polymer of Figs. 1 and 2. The method of calculation is described elsewhere [11]. The straight lines are drawn with the purpose of emphasizing regular trends in the discrete modes

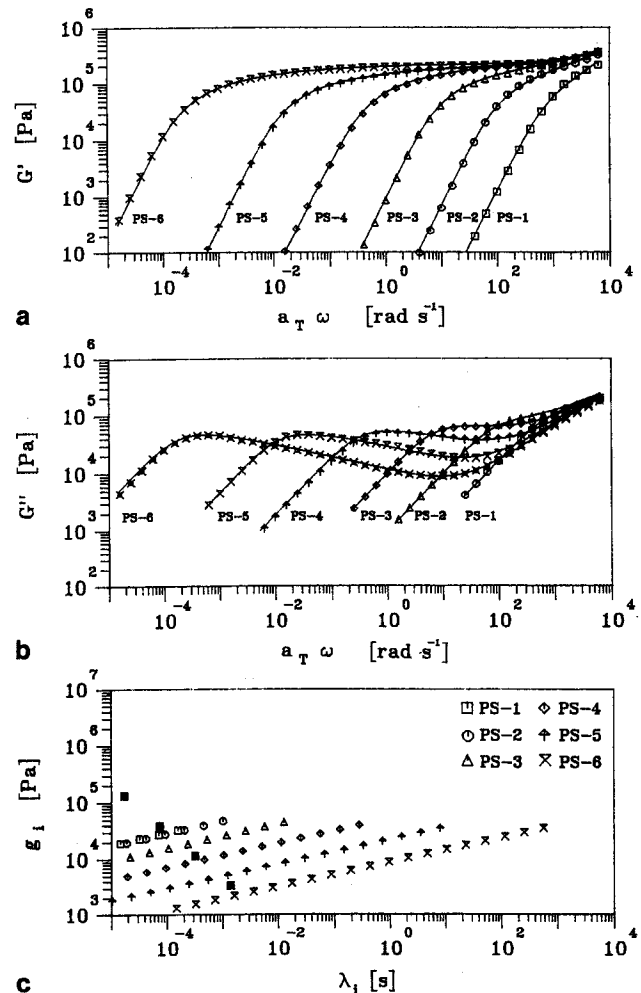


Fig. 4. a) Use of separate BSW- and CW-spectra for the flow and glassy regimes and their superposition to model the PS of Figs. 1 and 2. The points on the lines denote data points, the lines are the result of the fit, and the other points denote discrete relaxation modes  $g_i$ ,  $\lambda_i$ , as shown in Fig. 3. b) Loss modulus corresponding to Fig. 4a. c) Discrete BSW-spectra of the model polymer of Fig. 4a and b

Table 2. BSW-spectra and CW-spectra of the polystyrene standards PS-1 . . . PS-6 and polybutadiene PBD. The CW-spectrum is the same for all polystyrene standards

Sample	BSW-spectrum					CW-spectrum				
	$N_1$	$g_1$ [Pa]	$\lambda_1$ [s]	$n_1$ [-]	$a_1$ [-]	$N_2$	$g_2$ [Pa]	$\lambda_2$ [s]	$n_2$ [-]	$a_2$ [-]
PS-1	20	$3.35 \cdot 10^4$	$6.65 \cdot 10^{-3}$	0.22	0.45	5	$4.66 \cdot 10^5$	$4.02 \cdot 10^{-5}$	0.84	4.3
PS-2	20	$4.81 \cdot 10^4$	$1.03 \cdot 10^{-2}$	0.22	0.45	5	$4.66 \cdot 10^5$	$4.02 \cdot 10^{-5}$	0.84	4.3
PS-3	20	$4.60 \cdot 10^4$	$1.29 \cdot 10^{-1}$	0.22	0.45	5	$4.66 \cdot 10^5$	$4.02 \cdot 10^{-5}$	0.84	4.3
PS-4	20	$4.08 \cdot 10^4$	$2.80 \cdot 10^0$	0.22	0.45	5	$4.66 \cdot 10^5$	$4.02 \cdot 10^{-5}$	0.84	4.3
PS-5	20	$3.57 \cdot 10^4$	$8.07 \cdot 10^1$	0.22	0.45	5	$4.66 \cdot 10^5$	$4.02 \cdot 10^{-5}$	0.84	4.3
PS-6	20	$3.63 \cdot 10^4$	$5.70 \cdot 10^3$	0.22	0.45	5	$4.66 \cdot 10^5$	$4.02 \cdot 10^{-5}$	0.84	4.3
PBD	20	$3.28 \cdot 10^5$	$9.32 \cdot 10^1$	0.42	0.45	7	$1.13 \cdot 10^5$	$5.56 \cdot 10^{-5}$	0.34	4.3

Separation into a flow and a glassy regime [12] was implemented in a new program for determining separate spectra for each regime. Also implemented was the postulate that the modes sit on straight lines, as realized in Fig. 3. The first guess of the parameters  $g_i$ ,  $\lambda_i$  in the non-linear iterative procedure was taken from the shape of  $G''$  of PS-6. The discrete modes follow the  $G''$  curve in great detail. Then the minimization procedure determined the final values for the spectrum. The result, again, was an excellent fit of the data, see Figs. 4 and 5. Deviations between the spectra and the data are barely noticeable, even if the new approach does not reproduce any small waviness that might be in the data.

Most interesting is the regularity in the calculated relaxation modes  $g_i$ ,  $\lambda_i$ . The regular spacing and the alignment make it clear that the calculated spectra are power laws [11]. The spacing between the modes is ar-

bitrary for our purposes. The discrete spectra have the form

$$G(t) = \underbrace{\sum_{i=1}^{N_1} g_1 a_1^{n_1(i-1)} \exp\left(\frac{-t}{(a_1^{i-1} \lambda_1)}\right)}_{\text{flow regime}} + \underbrace{\sum_{i=1}^{N_2} g_2 a_2^{-n_2(i-1)} \exp\left(\frac{-t}{(a_2^{i-1} \lambda_2)}\right)}_{\text{glassy regime}} \quad (5)$$

The new parameters are listed in Table 2. No physical interpretation is given yet.

The result of the analysis is summarized by the following observations: the flow regime and the glassy regime can be separated into two additive components. Each component follows a simple power law.

### 3. Continuous relaxation spectrum

The spacing in the discrete spectra might be reduced until a continuous spectrum is found (see Appendix). The continuous spectrum  $H(\lambda)$  is conventionally defined by [2]

$$G(t) = \int_0^{\infty} \frac{H(\lambda)}{\lambda} e^{-t/\lambda} d\lambda \quad (6)$$

The result of the above analysis is a continuous spectrum:

$$H(\lambda) = \underbrace{H_1 \lambda^{n_1} h(1 - \lambda/\lambda_1)}_{\text{flow regime}} + \underbrace{H_2 \lambda^{-n_2} h(1 - \lambda/\lambda_2)}_{\text{glassy regime}} \quad (7)$$

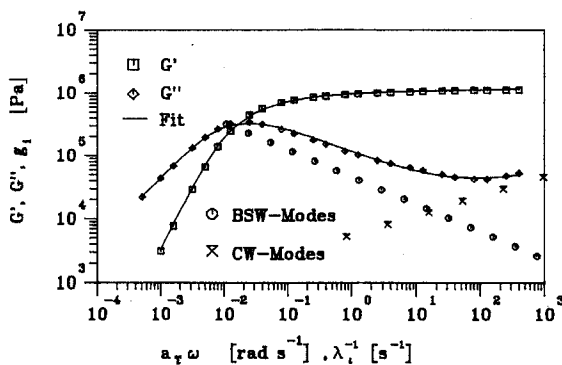


Fig. 5. Use of separate spectra for the flow and glassy regimes and their superposition to model the polybutadiene of Fig. 2. The points on the lines denote data points, the lines are the result of the fit, and the other points denote discrete relaxation modes  $g_i$ ,  $\lambda_i$ , as shown in Fig. 3

Table 3. Parameters of the continuous BSW-spectra for the polystyrene standards PS-1...PS-6 and polybutadiene PBD

Sample	$H_1 \lambda_{\max}^{n_1}$ [Pa]	$\lambda_{\max}$ [s]	$n_1$ [-]
PS-1	$4.20 \cdot 10^4$	$6.65 \cdot 10^{-3}$	0.22
PS-2	$6.02 \cdot 10^4$	$1.03 \cdot 10^{-2}$	0.22
PS-3	$5.76 \cdot 10^4$	$1.29 \cdot 10^{-1}$	0.22
PS-4	$5.11 \cdot 10^4$	$2.80 \cdot 10^0$	0.22
PS-5	$4.47 \cdot 10^4$	$8.07 \cdot 10^1$	0.22
PS-6	$4.55 \cdot 10^4$	$5.70 \cdot 10^3$	0.22
PBD	$4.11 \cdot 10^5$	$9.32 \cdot 10^1$	0.42

which requires a cut-off at the longest relaxation time of the flow regime,  $\lambda_1$ , and at some glass time  $\lambda_2$  for the glassy regime. This cut-off is introduced with a Heaviside function  $h(\cdot)$ .

The values of the parameters (Table 3) are related to the previously shown parameters of the discrete spectrum (Table 2). The reproduction of the  $G'$ ,  $G''$  data is exactly the same as with the geometrical series, Eq. (5).

The longest relaxation time varies with about the 3.4th power of the molecular weight (Fig. 6). The product  $H_1 \lambda_1^{n_1}$  is a material-specific constant. The variations in the calculated  $H_1$  value require further study (see below). The slopes  $n_1$  and  $n_2$  are material-specific constants, which are expected to depend somehow on molecular properties, such as chain flexibility, friction factor, or lateral chain dimension.

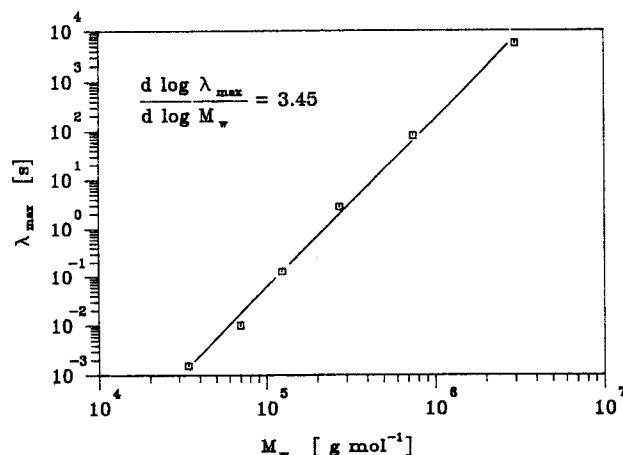


Fig. 6. Molecular-weight dependence of the longest relaxation time. The slope is about 3.45

#### 4. Properties of the ideal spectrum for the flow regime of LFM polymers

The parameters in the continuous spectrum are related to commonly used experimental parameters. In the following discussion, we will neglect the glassy contribution and concentrate on the flow regime. This ideal spectrum can be expressed in a more familiar notation:

$$H(\lambda) = n G_N^0 (\lambda/\lambda_{\max})^n h(1 - \lambda/\lambda_{\max}), \quad (8)$$

where  $G_N^0$  is the equilibrium modulus and  $\lambda_{\max}$  the longest relaxation time. We will call this the *BSW-spectrum*.

The relaxation modulus of the BSW-spectrum, as defined in Eq. (8), is an incomplete gamma function, which has to be determined numerically. The corresponding dynamic moduli

$$G'(\omega) = n G_N^0 \omega^2 \int_0^{\lambda_{\max}} (\lambda/\lambda_{\max})^n \frac{\lambda d\lambda}{1 + (\omega\lambda)^2} \quad (9)$$

and

$$G''(\omega) = n G_N^0 \omega \int_0^{\lambda_{\max}} (\lambda/\lambda_{\max})^n \frac{d\lambda}{1 + (\omega\lambda)^2} \quad (10)$$

are shown in Fig. 7 for the cases of  $n = 0.2, 0.3,$  and  $0.4$ . The plateau modulus is easily recovered for

$$\lim_{\omega \rightarrow \infty} G'(\omega) = G_N^0. \quad (11)$$

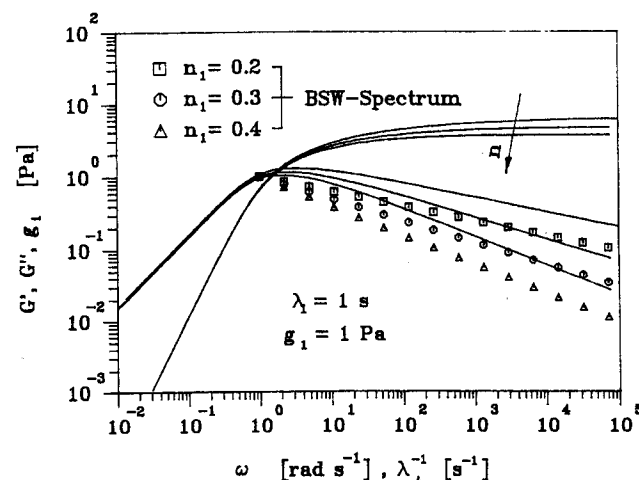


Fig. 7. Storage modulus and loss modulus as described by Eq. (8) with  $n = n_1$  (BSW-spectrum), i.e. neglecting the glass transition. The scaling parameter  $n_1$  is varied. A large  $n_1$  value lowers the curves in the entangled regime while the terminal zone is little affected. The curves are normalized by setting  $n_1 G_N^0 = 1$  Pa and  $\lambda_{\max} = 1$  s.  $n_1$  is the slope of  $G''(\omega)$  for  $\omega \rightarrow \infty$

Other properties of interest are the zero shear viscosity

$$\eta_0 = \lim_{\omega \rightarrow 0} \frac{G''(\omega)}{\omega} = \frac{n}{1+n} G_N^0 \lambda_{\max} \quad (12)$$

and the recoverable compliance

$$J_e^0 = \frac{1}{G_N^0} \left( 1 + \frac{1}{n^2 + 2n} \right) \quad (13)$$

These are just a few examples in which the BSW-spectrum relates linear viscoelastic parameters, as defined in the literature [2, 6].

An important relation is found for the intersect of the low-frequency asymptotes of  $G'$  and  $G''$ . These asymptotes intersect at a frequency

$$\omega_0 = \frac{1}{\lambda_{\max}} \frac{n+2}{n+1} = \frac{\int_0^{\infty} G(t) dt}{\int_0^{\infty} t G(t) dt} \quad (14)$$

This is an expression that occurs in many linear viscoelastic-flow problems [5].

It is interesting to note that all of the conventionally studied material functions disguise the power-law character of the spectrum. Only by detailed analysis, can we find the underlying pattern, which is presented here.

The BSW-spectrum, having a positive power-law exponent, obviously is *unrelated* to the Chambon-Winter spectrum [13–15], which has a negative exponent. Obviously,  $\tan \delta$  varies over the entire frequency range and no relation exists to liquid/solid transitions.

### 5. Spectrum for the glass transition

The power-law spectrum with negative exponent (CW-spectrum),  $H(\lambda) = H_2 \lambda^{-n_2}$  has been proposed by Chambon and Winter [13–15] for describing liquid/solid transitions in crosslinking polymers, and its properties have been studied extensively. It was surprising to see that the same spectrum seems to reappear in this very different context. From crosslinking polymers, we know that the CW-spectrum of the critical gel is cut off by a characteristic *lowest* relaxation time (high frequency limit). Something similar is expected for the transition behavior here.

The main phenomenological difference compared with the critical gel is that the longest relaxation time

does not diverge to infinity. Instead, it is determined by the flow regime, which cuts off the CW-spectrum at its low frequency end. Molecular differences are obvious, because the critical gel is highly branched and infinitely broad in its molecular-weight distribution. This shows that the common properties are not based on molecular details. The CW-spectrum seems to be of broader importance, beyond the specific case of gelation. Additional experiments are needed before drawing conclusions about this very interesting observation. The main focus of this study is really on the flow regime and not on the glassy behavior.

### 6. Comparison with Rouse and Doi-Edwards spectra

The Rouse spectrum can be reconsidered in the new context. The shape of the  $G', G''$ -plot (for instance in [2]) clearly shows, that the Rouse model describes the terminal zone very well. However, it then continues directly into the glassy region without allowing a plateau modulus at intermediate frequencies. Such behavior is typical for LFM polymers of low molecular weight  $M$  near the entanglement limit  $M_c$ . For this class of polymers, the Rouse model is ideal and it has to be considered a remarkable success that the entire range from flow into the glass regime can be represented in such a clear format.

This observation agrees well with the known success of the Rouse model when it comes to predicting the molecular-weight dependence of the zero shear viscosity to be linear,  $\eta_0 \sim M$  for  $M \approx M_c$ .

Reproduction of the actual data (of PS-1, for instance) might require a slight change of the Rouse model for accommodating the specific slope of the CW-spectrum. This slope is denoted as  $n_2$  in Eq. (7). The modified Rouse model has the form

$$G(t) = g \sum_{i=1}^N \exp(-ti^{1/n_2}/\lambda_{\max}) \quad (15)$$

referring to the notation of Eq. (1). The meaning of the additional parameter is not clear as of now.

In comparison, the de Gennes-Doi-Edwards spectrum [3, 4] applies to the flow regime (excluding the transition to the glass). This already presents a significant difference compared with the Rouse spectrum. The further comparison with the BSW-spectrum is very interesting (see Fig. 8). While the agreement is about perfect in the terminal zone, principally different  $G', G''$  curves are found in the rubbery zone, which reflects the dynamics of the polymer chain. The

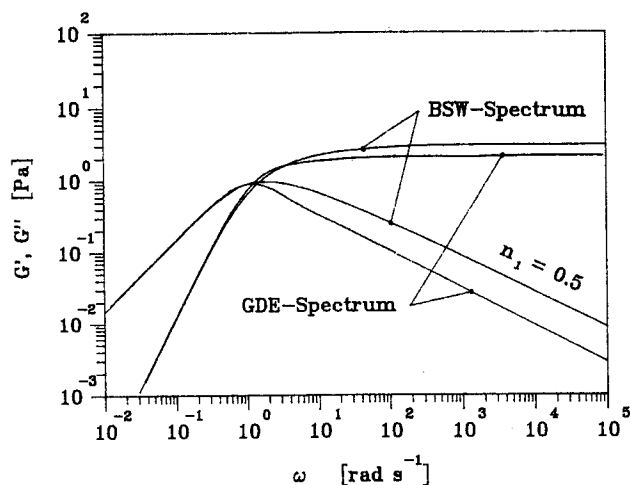


Fig. 8. Comparison of dynamic moduli of GDE-spectrum [3, 4] and of BSW-spectrum [Eq. (8)]

differences even remained when we chose a value of 0.5 for the scaling parameter  $n_1$  (for accommodating the  $G''$  slope of the GDE-spectrum at high frequency).

### 7. Application to bimodal distributions

The ideal behavior of LFM-polymers is not only of basic physical importance, but it will help to solve applied problems. This is demonstrated with the relaxation behavior of a binary mixture of PS3 and PS5, as measured by Schausberger et al. [9]. The dynamic moduli of the blend are modeled by two superimposed BSW-spectra, for which the shift is determined by means of Schausbergers mixing rule [14]. The contribution to the glass transition is added in a separate second step [12]. The agreement between measurement and prediction is excellent (see Fig. 9 and Table 4). This suggests possible applications of the BSW-spectrum in mixing rules for polydisperse polymers.

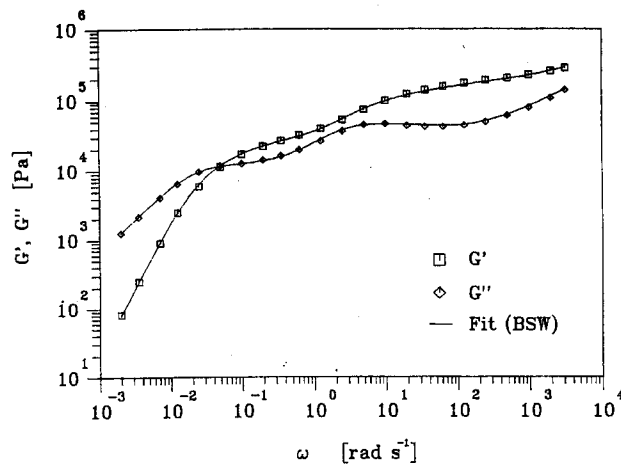


Fig. 9. Dynamic modulus of 50% mixture of PS-3 and PS-5, as measured by Schausberger et al. [9]. The relaxation behavior is described by a superposition of two continuous spectra, Eq. (7), by means of a mixing rule [14]

### 8. Discussion

The linear chains show scaling behavior both in the flow regime and in the transition to the glass. The simplicity of the result and the realistic prediction of observable linear viscoelastic material functions of LFM polymers suggest that the proposed relaxation spectrum is of more general importance, beyond the specific samples of this analysis.

In the analysis, little emphasis was given to the glassy behavior, because not enough high-frequency data are available to us (we have not yet looked for such data). However, the onset of a power-law region is suggested here (CW-spectrum). This is not completely unreasonable, because power law relaxation  $G(t) = St^{-n}$  is known to govern other types of liquid-solid transitions in polymers.

Subtraction of the glassy contribution from the measured  $G', G''$  curves exposes the flow region

Table 4. BSW-spectrum and CW-spectrum of the blend of 50% PS-3 and 50% PS-5. Note that the CW-spectrum is identical to the ones of the standards (Table 2). The BSW-spectra for the components PS-3 and PS-5 are shifted with the slope  $n_1$  and the spacing  $a_1$  remains unchanged

Sample	BSW-spectrum					CW-spectrum				
	$N_{1,i}$	$g_{1,i}$ [Pa]	$\lambda_{1,i}$ [s]	$n_{1,i}$ [-]	$a_1$ [-]	$N_2$	$g_2$ [Pa]	$\lambda_2$ [s]	$n_2$ [-]	$a_2$ [-]
PS-3	20	$3.22 \cdot 10^4$	$3.58 \cdot 10^{-1}$	0.218	0.45	5	$4.66 \cdot 10^5$	$4.02 \cdot 10^{-5}$	0.893	4.3
PS-5	20	$8.64 \cdot 10^3$	$4.37 \cdot 10^1$	0.218	0.45	0	0	0	0	0

towards higher frequencies. The subtraction is especially successful for the higher molecular-weight samples, while it introduces more substantial error in the spectra of samples with lower molecular weight. This might be a reason for the large sample-to-sample fluctuations of  $H_1 \lambda_{\max}^{n_1}$  (which should really be a constant material parameter). The small, but finite width of the molecular-weight distribution in the samples cannot be blamed for the sample-to-sample variations of  $H_1$ , because it would not lower the plateau modulus of a polymer.

Really surprising for us was the fact that such ideal relaxation behavior was seen with all samples. Relaxation does not seem to be sensitive to small deviations from perfect monodispersity. These deviation, however, might affect the value of  $n_1$ .

The study shows a close relation between relaxation spectra in discrete and continuous form. Either choice leads to the same results. This gives a large amount of flexibility in the data analysis, a fact which does not seem to find enough appreciation in the published literature.

## 9. Conclusions

We propose that monodisperse linear polymer melts have a unique relaxation spectrum (BSW-spectrum) which is of the form  $H(\lambda) = H_1 \lambda^{n_1} \cdot h(\lambda - \lambda_{\max})$ .  $H_1$  and  $n_1$  are polymer specific and  $\lambda_{\max}$  is the longest relaxation time, which cuts off the spectrum at low frequencies. The glass transition at high frequencies is described by a CW-spectrum, a power-law spectrum of form the  $H(\lambda) = H_2 \lambda^{-n_2}$ . For real materials, both spectra were simply superimposed to find a good description of the transition region.

The scaling exponent of the BSW-spectrum  $n_1$  was found to be substantially different for the two polymer species available to us. This implies that no universal shape exists for  $G'$ ,  $G''$  of LFM polymers, a result that should have a large effect on theory. It seems that an important parameter is missing in a theory of chain dynamics, which predicts material-independent linear-viscoelastic functions of LFM polymers. Ideally monodisperse samples are needed to substantiate this finding.

The proposed spectrum comes strictly from experimental observation and is not biased by any theoretical preference. This will make it a good measure for new theoretical developments. Knowledge of the spectrum will also allow checking the many empirical interrelations [2] that have been proposed for linear viscoelastic functions.

We do not know a suitable physical model for explaining the observed relaxation spectrum. However, the power-law form of the BSW-spectrum, Eq. (8), suggests that there is a scaling relation between all relaxation modes [3, 4]. This includes the short modes, associated with the chain ends or segments, and the longer modes of the connected part of the chain. While we possibly might know the relaxation of a linear flexible chain, we still have to find its motion mechanism.

## Appendix A

### Interrelations between continuous and discrete spectra

The continuous relaxation spectrum

$$H(\lambda) = H_1 \lambda^{n_1} h(1 - \lambda/\lambda_{\max}) \quad (\text{A } 1)$$

can be expressed as an infinite series. From a quantitative point of view, both representations are identical. Exemplary, the interrelation shown for  $G''(\omega)$  is

$$G''(\omega) = \int_{-\infty}^{\infty} H(\lambda) \frac{\omega \lambda}{1 + \omega^2 \lambda^2} d \ln \lambda, \quad (\text{A } 2)$$

which transforms to

$$G''(\omega) = \int_{-\infty}^{\ln \lambda_{\max}} H_1 e^{n_1 \ln \lambda} \frac{\omega e^{n_1 \ln \lambda}}{1 + \omega^2 e^{n_1 \ln \lambda}} d \ln \lambda \quad (\text{A } 3)$$

for the BSW-spectrum [Eq. (A 1)]. Numerical integration of Eq. (A 3) leads to an infinite series (an analytic solution is not known to us):

$$G''(\omega) = \sum_{i=0}^{\infty} H_1 (-\ln a) \lambda_{\max}^{n_1+1} a^{i(1+n_1)} \times \frac{\omega}{1 + \omega^2 \lambda_{\max}^2 a^{2i}}. \quad (\text{A } 4)$$

Parameter  $a$  is related to the step size in the numerical integration above, so that

$$a = e^{-\Delta \ln \lambda}, \quad 0 < a < 1. \quad (\text{A } 5)$$

Alternatively, the discrete spectrum might be expressed as a sum of exponential decays, and Eq. (A 2) becomes [2]



$$G''(\omega) = \sum_{i=0}^{\infty} g_i \frac{\omega \lambda_i}{1 + \omega^2 \lambda_i^2} \quad (\text{A6})$$

Comparison of Eq. (A6) with Eq. (A4) gives the desired result. The relaxation modes of the discrete spectrum  $g_i$ ,  $\lambda_i$  are scaled in the geometric series

$$g_i = g_0 a^{in_1}, \quad g_0 = H_1(-\ln a) \lambda_{\max}^{n_1}, \quad (\text{A7})$$

and

$$\lambda_i = \lambda_0 a^i, \quad \lambda_0 = \lambda_{\max}. \quad (\text{A8})$$

Scaling relations in Eqs. (A7) and (A8) are universal. They are equally found by solving the integral equations for  $G'(\omega)$  or  $G(t)$ .

The leading relaxation strength of the discrete spectrum depends on the spacing of the relaxation modes. However, the longest relaxation time is invariant and is identical to the cut-off relaxation time of the continuous spectrum. A change in the spacing,  $a$ , does not alter the shape of the  $G''$  curve; however, its waviness increases with a wider spacing.

#### Acknowledgments

M. Baumgaertel und H.H. Winter gratefully acknowledge the support of the Material Research Laboratory (MRL) of the University of Massachusetts and of the Massachusetts Center of Excellence together with General Electric Plastics Division. We thank Dr. R. Colby for supplying tabulated data from his PhD thesis. A. Schausberger acknowledges the support of the University of Linz during his sabbatical. Only the merging of two very different research philosophies between Linz and Amherst made this study possible.

#### References

1. Rouse PE (1953) J Chem Phys 21:1272
2. Ferry JD (1980) Viscoelastic properties of polymers. Wiley, New York
3. de Gennes PG (1979) Scaling concepts in polymer physics. Cornell Univ Press, Ithaca
4. Doi M, Edwards SF (1986) The theory of polymer dynamics. Clarendon Press, Oxford
5. Bird RB, Armstrong RC, Hassager O, Curtis CE (1977) Dynamics of polymeric liquid. Wiley, New York
6. Graessley WW (1982) Adv Polym Sci 47:67
7. Larson R (1987) Constitutive equations for polymer melts and solutions. Butterworths, London
8. Onogi S, Masuda T, Kitagawa K (1970) Macromolecules 3:109
9. Schausberger A, Schindlauer G, Janeschitz-Kriegl H (1985) Rheol Acta 24:220
10. Colby RH (1985) PhD Thesis. Northwestern University
11. Baumgaertel M, Winter HH (1989) Rheol Acta 28:511
12. Schausberger A (1991) to be published
13. Chambon F, Winter HH (1985) Polym Bull 13:499
14. Winter HH, Chambon F (1986) J Rheol 30:367
15. Chambon F, Winter HH (1987) J Rheol 31:683
16. Schausberger A (1986) Rheol Acta 25:596

(Accepted September 25, 1990)

#### Authors' addresses:

Dipl.-Ing. M. Baumgaertel and Prof. H.H. Winter  
Department of Chemical Engineering  
University of Massachusetts  
Amherst, MA 01003, USA

Dr. A. Schausberger  
Physikalische Chemie  
Johannes-Kepler-Universität  
4040 Linz, Austria